0273-2289/95/5152—0785$06.60

Evaluation of Bacterial Detachment Rates in Porous Media

B. M. PEYTON,* R. S. SKEEN,
B. S. HOOKER, R. W. LUNDMAN, AND A. B. CUNNINGHAM
Pacific Northwest Laboratory, Richland, WA 99352

ABSTRACT

The ability of published biomass detachment rate expressions to describe experimental data obtained from porous media reactors using *Pseudomonas aeruginosa* grown aerobically on glucose was evaluated. A first-order rate expression on attached biomass concentration best reflected effluent substrate concentration for combined data sets. Detachment rate coefficient k_{d1} was dependent on initial substrate concentration. Simulation of porous media reactor experiments indicated that responses using higher influent substrate concentrations possessed greater sensitivity to variations in k_{d1}. Simulations of field bioremediation systems suggest the use of accurate biofilm development kinetics is important in the prediction of well bore biofouling.

Index Entries: *In situ* bioremediation; biofilm; simulation; detachment rate; attachment rate.

Nomenclature: C_a, concentration of a dissolved chemical in the liquid phase (M/L^3); C_{ai}, initial concentration of a dissolved chemical in the liquid phase (M/L^3); D_a, dispersivity of a dissolved chemical in the liquid phase (L^2/t); D_x, dispersivity of biomass in the liquid phase (L^2/t); k_a, biomass attachment coefficient (L/t); k_{d1}, biomass detachment coefficient (units are expression dependent); k_{d2}, biomass detachment coefficient (units are expression dependent); K_s, Monod half-saturation coefficient (M/L^3); r_a, biomass attachment rate ($M_X/L^2/t$); r_d, biomass detachment rate ($M_{Xf}/L^2/t$); r_g, rate of liquid-phase biomass growth ($M_X/L^3/t$); r_g^f, rate of attached-phase biomass growth ($M_{Xf}/M_k/t$); t, time (t); v, Darcy velocity (L/t); X, biomass concentration in the liquid phase (M_X/L^3); X_f, biomass concentration in the attached phase (M_{Xf}/M_k^1); $Y_{X/C}$, biomass observed yield (M_X/M_c); z, distance from the reactor inlet (L).

*Author to whom all correspondence and reprint requests should be addressed.

Greek Symbols: ϵ, volume fraction of the media filled with liquid (unitless); η, effectiveness factor for biofilm substrate consumption (unitless); μ, specific growth rate of biomass (t^{-1}); μ_m, maximum specific growth rate of biomass (t^{-1}); ρ_k, substratum bulk density, M_k/L^3).

INTRODUCTION

In situ bioremediation relies on developing and maintaining microbial activity in contaminated regions. Distributing this activity more evenly throughout the subsurface depends on the ability to engineer systems that spatially distribute microbial activity. The main limitation to achieving this goal is the inability to disperse injected fluids evenly throughout the subsurface using recirculation wells. This situation results from the radial flow patterns that emanate from these wells because fluid velocity diminishes rapidly with distance. Hence, injected nutrients tend to react near the well bore, limiting the microbial activity at remote points in the flow field. This phenomena has been observed both in the laboratory (*1*) and in the field (*2*).

To extend the biologically active region, researchers have focused on developing nutrient feeding strategies that minimize near-well growth to allow substrate transport further from the injection point (*2–5*). For example, Shouche et al. (*3*) used simulations of a one-dimensional flow field to determine a strategy for pulsed feeding of electron donor (acetate) to minimize biomass growth near the field inlet. This was accomplished by adjusting the acetate concentration, the duration of the feed pulse, and the length of time between feed pulses. The maximum biomass concentration achieved in a 2-m soil column during 50 d of operation could be reduced by more than an order of magnitude as compared to a base case representing the pulsing strategy used in the field work of Semprini et al. (*2*). Roberts et al. (*4*), in similar studies, determined that well bore biofouling could be minimized through the use of separate injection pulses of electron donor and electron acceptor. Neither of these investigations accounted for the movement of microorganisms, but considered active biomass as a fixed film. In fact, most reported simulations of *in situ* bioremediation do not incorporate the processes of bacterial attachment and detachment (*6–8*).

A limited number of investigations have attempted to describe bacterial transport in porous media through attachment and detachment rate expressions (*9–13*). For prediction of *in situ* bioremediation activity, this is necessary because contaminant transformation is a direct result of the presence of the subsurface biomass, and the spatial distribution of biomass is affected by bacterial attachment and detachment. The goal of this article

is to evaluate the ability of current detachment rate expressions to describe biofilm dynamics in porous media. In addition, the sensitivity of simulated biomass profiles to detachment rate is examined for a porous media column reactor and a field-scale *in situ* remediation system.

METHODS

A pure culture of *Pseudomonas aeruginosa* was used to inoculate porous media reactors. This species is known to form biofilms and has well-characterized kinetic parameters (*14,15*). Before inoculating the reactors, the bacteria were grown aerobically on glucose at 35°C for 2 d in batch culture. This resulted in an inoculum cell concentration of approx 10^7 cells/mL.

A 50-mm long × 31-mm diameter reactor was packed with 1-mm glass beads. Wall effects were minimized by using a bed-to-particle diameter ratio of ≥30, as recommended by Cohen and Metzner (*16*). The packing was held in the reactor with #30 brass gauze positioned at each end. Liquid sampling ports and conductivity ports were provided at each end of the reactor at the brass gauze–bead interface. Glucose and mineral salts solutions, stored in separate carboys, were diluted with sterile, aerated, distilled water before being continuously fed to the column. Mineral salts media used in these experiments have been described by Siebel and Characklis (*15*). Glucose solution flow rates were adjusted to give column influent concentrations of either 2.3 or 19.7 mg/L. Stoichiometric calculations based on oxygen-saturated water and effluent glucose concentrations indicate that the reactor was not oxygen-limited at the higher substrate loading. Before inoculation, the reactor and feed apparatus were steam-sterilized for 1 h at 18 psig and 125°C. Once sterile and assembled, the reactor was isolated with tubing clamps and inoculated with *Ps. aeruginosa*. After 4 h, the clamps were removed and the reactor was operated in an up-flow mode at a constant flow rate of 38 mL/min at a temperature of 20°C. Each experiment was operated for at least 12 d.

Influent and effluent cell samples were collected daily and preserved in buffered formalin prior to analysis. Suspended cells were stained with either Hoechst 33342 or DAPI fluorescent stains, although DAPI was primarily used because it was less susceptible to fading during exposure to UV light. Cell concentrations were measured using epifluorescent enumeration.

Influent and effluent glucose samples were also collected daily. Once collected, the glucose samples were centrifuged to remove any cells and extracellular polymeric substances (EPS). Glucose samples were analyzed colorimetrically using Sigma Diagnostics® enzymatic glucose determination (procedure 510), modified for measurement at lower concentrations.

Table 1
Model of Nutrient and Biomass Transport
and Biofilm Accumulation in Porous Media

Substrate

$$(\partial C_a / \partial t) = D_a (\partial^2 C_a / \partial z^2) + (D_a / \epsilon)(\partial \epsilon / \partial z)(\partial C_a / \partial z) - (v / \epsilon)(\partial C_a / \partial z) - (C_a / \epsilon)(\partial \epsilon / \partial t) - [r_g / Y_{x/c}] - [r_g^f \rho_k / \epsilon Y_{x/c}] \quad (1)$$

Suspended biomass

$$(\partial X / \partial t) = D_x (\partial^2 X / \partial z^2) + (D_x / \epsilon)(\partial \epsilon / \partial z)(\partial X / \partial z) - (v / \epsilon)(\partial X / \partial z) - (X / \epsilon)(\partial \epsilon / \partial t) - r_a + (r_d \rho_k / \epsilon) + r_g \quad (2)$$

Attached biomass

$$(d X_f / d t) = (r_a \epsilon / \rho_k) - r_d + r_g^f \quad (3)$$

where

Suspended growth rate

$$r_g = \mu X = [(\mu_m C_a / K_s + C_a)] X \quad (4)$$

Attached growth rate

$$r_g^f = \mu X_f = [(\mu_m C_a / K_s + C_a)] X_f \quad (5)$$

Attachment rate

$$r_a = k_a X \quad (6)$$

Detachment rate expressions are given in Table 2.
Constants and parameter values are given in Table 3.

MODEL DEVELOPMENT

The equations used to describe nutrient and biomass transport, and biofilm accumulation in the porous media reactor are presented in Table 1. Biofilm development involves a combination of phenomena, including biomass growth in the aqueous phase (r_g), growth in the biofilm (r_g^f), and interfacial mass transfer through processes of attachment (r_a) and detachment (r_d). Changes in soil porosity and biofilm thickness are described by the method of Taylor and Jaffe (*17*). Values of porosity were calculated using the cut and random rejoin method of Taylor et al. (*27*), whereas the partial differentials of porosity with time and position were evaluated using a backward finite difference method. Biomass attachment rate was modeled as a first-order process (Eq. [6]), similar to that used by Taylor and Jaffe (*9*), and is based on conservative particle filtration theory (*18*). The effects of porosity changes on the attachment rate were neglected, since simulation results were insensitive to attachment rate and porosity changes would only account for a maximum of 15% of the total attachment rate. The detachment rate expressions evaluated in this study, shown in the second column of Table 2, are representative of rate expres-

Table 2
Detachment Rate Expressions and Optimum Coefficient Values Obtained

Eq. #	Expression[a]	Low substrate loading k_{d1}	k_{d2}	SSE	High substrate loading k_{d1}	k_{d2}	SSE	Reference
(7)	$k_{d1} X_f$	0.00098	—	0.43	0.0044	—	18	Chang and Rittman, 1988 (*11*) Kreikenbohm and Stephan, 1985 (*19*) Rittman, 1989 (*20*)
(8)	$k_{d1} X_f^2$	2.3	—	3.4	6.2	—	480	Bryers, 1987 (*12*) Trulear and Characklis, 1982 (*21*) Wanner and Gujer, 1986[b] (22)
(9)	$k_{d1} \mu \eta X_f$	0.55	—	0.27	0.84	—	120	Speitel and DiGiano, 1987[b,c,d] (*10*)
(10)	$k_{d1} \mu \eta X_f^2$	2600	—	2.8	1400	—	470	Stewart, 1993[b,c,d] (*13*)
(11)	$k_{d1} X_f + k_{d2} \mu \eta X_f$	0.00064	0.21	0.21	0.0044	.001	18	Speitel and DiGiano, 1987[b,c] (*10*)
(12)	$k_{d1} X_f + k_{d2} \mu \eta X_f^2$	0.00098	0.026	0.43	0.0043	110	14	Stewart, 1993[b,c] (*13*)

[a] The specific growth rate, μ, was calculated by standard Monod kinetics, shown in Eqs. (4) and (5).
[b] Assuming biofilm density is constant.
[c] Referenced authors assumed $\eta = 1$.
[d] If $k_{d2} = 0$.

Table 3
Parameter Values Used in the Solution of Eqs (1–12)

Parameter	Symbol	Value	Units
Dispersion coefficient	D = av	25	cm^2/min
Dispersivity	a	5.0	cm
Velocity	v	5.0	cm/min
Porous media bulk density	ρ_k	1600	kg/m^2
Biomass yield	$Y_{x/c}$	0.46	mg X (mg C_a)$^{-1}$
Maximum specific growth rate	μ_m	6.7×10^{-3}	min^{-1}
Half saturation coefficient	K_s	5.0	mg/L
Attachment rate coefficient	K_a	0.38	min^{-1}
Initial porosity	ϵ	0.40	L liquid (L total)$^{-1}$

sions found in literature *(9–13,19–22)*. Parameter and coefficient values are given in Table 3.

Numerical simulation of the porous media reactor system used an explicit finite-difference algorithm to reflect one-dimensional spatial variation, whereas time derivatives were estimated using the Runge-Kutta-Feldberg method. Experimental data were used to determine optimum values for detachment rate parameters using the generalized-reduced-gradient optimization method available in Simusolv® version 2.0 optimization software (Dow Chemical Co., Midland, MI). Optimum detachment rate coefficients were chosen by minimizing the standard error between model estimates and experimental data.

Field-scale numerical simulations in this work used a modification of the multidimensional ReActive Flow and Transport code (RAFT) developed by Wheeler et al. *(8,23,24)*. This code uses a mixed finite-element method to calculate pressure, velocity, and concentration profiles in the flow field for convection-dominated transport problems. A time-splitting procedure is employed to provide a stable solution of the transport and biodegradation equations. Transport equations are solved by the modified method of characteristics, whereas microbial reactions are described in a system of ordinary differential equations solved using a fourth-order Runge-Kutta technique. The simulated, two-dimensional flow field was 2.75 m on a side with a single, central injection well. The flow field was assumed initially to contain no glucose and an attached biomass concentration of 1.0 mg dry biomass/kg of soil (mg DW/kg soil). This concentration is based on an initial concentration of 6×10^6 CFU/g soil.

RESULTS AND DISCUSSION

Figure 1A and B shows the experimentally measured and simulated effluent substrate concentrations for the porous media reactor. Influent substrate concentrations of 2.3 and 19.7 mg/L are represented in Figs. 1A

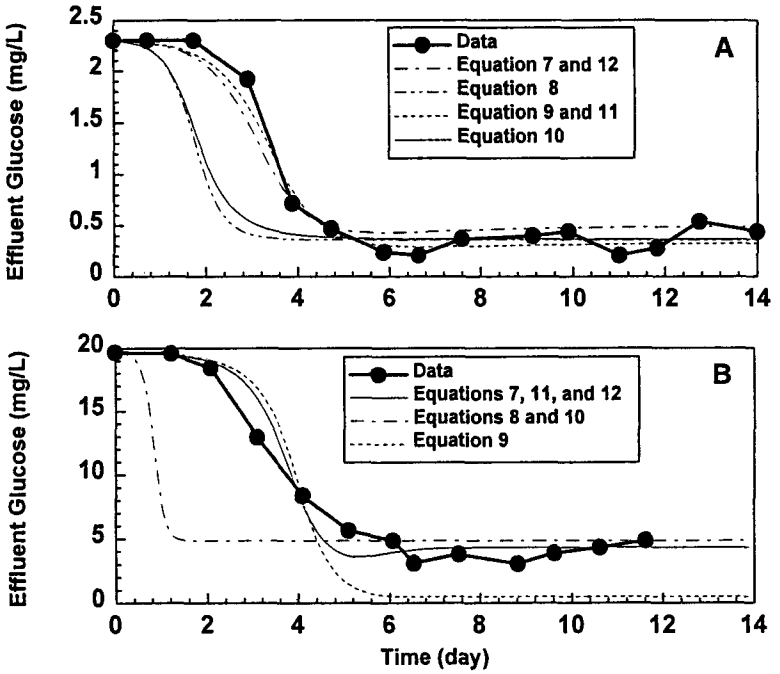

Fig. 1. Comparison of various detachment rate expressions optimized to give the best possible fit of experimental data obtained for influent substrate concentrations of (**A**) 2.3 mg/L and (**B**) 19.7 mg/L.

and B, respectively. A value of 0.38 min^{-1} was used for the k_a in all simulations represented in Fig. 1. Early simulation optimizations (not presented) indicated that 0.38 min^{-1} (22.8 h^{-1}) was a reasonable attachment rate coefficient and that simulation results were very insensitive to the value of the attachment rate coefficient. A change in the coefficient value of an order of magnitude in either direction had little effect on the predicted results. A similar optimized value of 0.214 min^{-1} (12.8 h^{-1}) was found by Taylor and Jaffe (*9*). The simulated results demonstrate the best fit for the data for each of the detachment equations shown in Table 2. All detachment expressions reasonably reflect experimental data for an inlet substrate concentration of 2.3 mg/L, but as shown in column 5 of Table 2, Eqs. (7), (9), (11), and (12) give values for sum squared errors (SSE) that are significantly lower than those for Eqs. (8) and (10). For an inlet substrate concentration of 19.7 mg/L, only detachment Eqs. (7), (11), and (12) accurately represent the experimental data. This trend can be seen from the SSE data in column 8 of Table 2. For the high substrate loading data, the SSE for Eqs. (11) and (12) are essentially the same as given by Eq. (7), because the second terms in Eqs. (11) and (12) do not significantly improve the overall fit, representing < 0.1 and 10% of the overall detachment rate, respectively.

These results demonstrate that the first-order detachment equation best represents the combined data sets. In contrast, Eqs. (8) and (10) do not accurately describe either case, Eq. (9) is applicable only to low substrate loading data, and Eqs. (11) and (12) are essentially the same as Eq. (7) for the high substrate loading case. It is also apparent from estimates of k_{d1} in Eq. (7) that a single value of this parameter does not describe both data sets. The value that best represents low substrate data is 9.79×10^{-4}/min (0.0587 h^{-1}), whereas a value of 4.4×10^{-3}/min (0.264 h^{-1}) best represents the high substrate data. Hence, although the first-order model can describe individual experiments, it cannot be used as a predictive expression for variable substrate loadings. This result is consistent with previous observations showing that detachment rate coefficients increase with inlet substrate concentration (*25*). Because the model is not globally predictive, the sensitivity of simulated results for both the reactor and an *in situ* bioremediation flow field to the detachment rate was further examined to determine the effects of this parameter on *in situ* bioremediation design. Only the detachment rate coefficient was examined because initial calculations revealed that the simulated results were much more sensitive to detachment rate. In fact, a 100% increase in the attachment rate coefficient was offset by only a 4% increase in the detachment rate coefficient.

Figure 2A shows the predicted behavior of the 2.3 mg/L experiment using detachment Eq. (7) and values of k_{d1} that are between 0.5 and 2.0 times the optimum value. It can be seen that levels of k_{d1} between 0.5 and 1.25 times the optimal level give a reasonable prediction of the data. However, larger k_{d1} values significantly over-predict the detachment rate, which results in less attached biomass in the column and higher substrate levels in the effluent. Similar data for the 19.7 mg/L case are shown in Fig. 2B. Results of these simulations indicate a greater sensitivity to variations in k_{d1} at higher influent substrate concentrations, since only the optimum value of k_{d1} accurately reflects the data. A value for k_{d1} that is one-half of the optimum severely underpredicts the detachment rate, causing more substrate consumption than was measured experimentally. When k_{d1} was raised to 1.25 times the optimum value, complete washout of the attached biofilm ensued.

To estimate the effects of the detachment rate coefficient on a field bioremediation system, the biofilm kinetic equations were applied to a two-dimensional, radial flow geometry with a central injection well. The field simulations represent a Department of Energy Hanford Site carbon tetrachloride (CCl_4) plume. The soil is very sandy with low native organic carbon. A detailed site characterization indicates that most of the contaminant is dissolved in the ground water, rather than adsorbed to the sediments. In addition, the installed bioremediation system will have a high recycle rate when compared to the overall contaminant reaction rate and will, therefore, have a significant amount of contaminant ($\sim$2/mg/L)

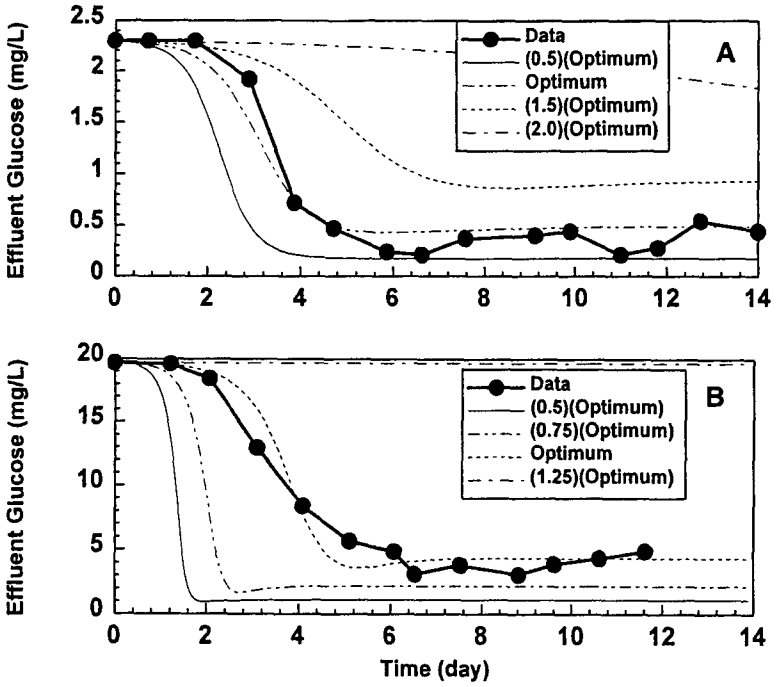

Fig. 2. Sensitivity of predicted effluent substrate concentration to the detachment rate coefficient used in Eq. (7) for influent substrate concentrations of (**A**) 2.3 mg/L and (**B**) 19.7 mg/L.

reinjected into the formation with the nutrients. An influent substrate concentration of 19.7 mg/L at a flow rate of 27.25 $m^3/d/m$ of well screen was used for these simulations. In addition, a contaminant was assumed present in the influent at a concentration of 2 mg/L. Contaminant destruction kinetics were first-order in biomass and contaminant concentration, based on expressions for carbon tetrachloride destruction reported by Hooker et al. (*26*). Although these expressions are not applicable to aerobic growth of *Ps. aeruginosa* on glucose, they are typical for cometabolically degraded contaminants, and provide insight to the sensitivity of *in situ* bioremediation to bacterial transport. Predicted biofilm profiles after 38 d for various k_{d1} values are shown in Fig. 3A as a function of distance from the injection well. Values of k_{d1} were chosen to reflect ±25% of the optimum level determined for the high substrate feed rate in porous media reactor studies.

It is apparent from Fig. 3A that the value of the detachment coefficient affects the spacial distribution of biomass. Increased bacterial detachment results in less biomass near the injection well and a more uniform profile throughout the flow field. However, these differences in biomass profiles have little effect on the total amount of contaminant destroyed in the flow field. This result can be seen in Fig. 3B, which represents field effluent contaminant concentration as a function of time for

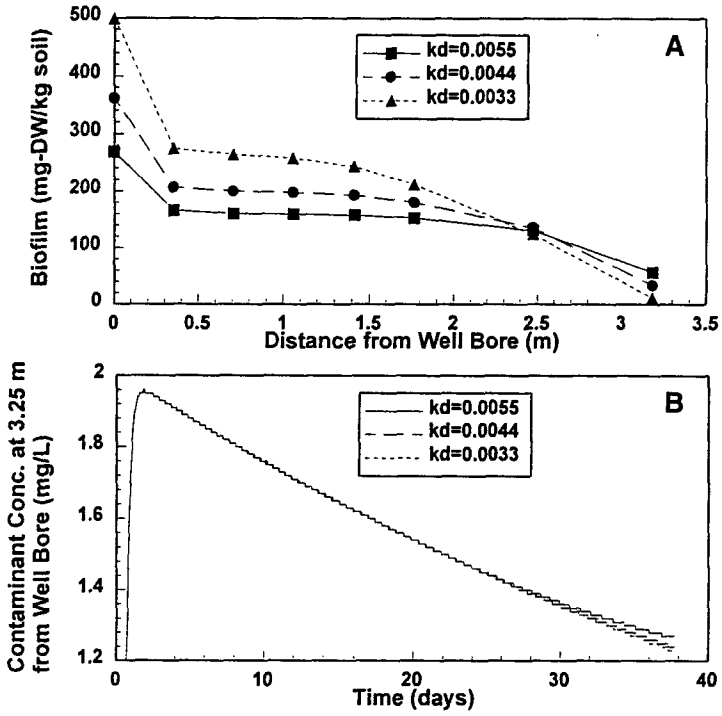

Fig. 3. Sensitivity of predicted (**A**) biomass distribution and (**B**) contaminant concentration to the detachment rate coefficient used in Eq. (7), under radial flow conditions for an influent substrate concentration of 19.7 mg/L.

the three values of k_{d1}. The effluent concentration after 38 d of operation is approx 1.24 mg/L in all cases. This inference is further supported by the fact that all three cases had nearly identical substrate concentration profiles after 38 d, with all glucose consumed within the first 0.7 m. It should be noted that these results neglect adsorption of contaminant to the solid phase. If contaminants were strongly adsorbed, then a more uniform biomass profile would result in less spacial variation in destruction rates.

Although the integrated microbial reaction characteristics for the flow field are not highly sensitive to detachment rate, it is necessary to include this parameter to account for near well accumulation of biomass and biofouling. If detachment rate is neglected and biomass is considered a fixed film for simulations of 19.7 mg/L glucose injection to the flow field, complete biofouling is predicted after approx 8 d. In contrast, if the detachment rate applied to this simulation is conservatively increased to the level observed using the 2 mg/L data from the porous media reactor, a near-well, steady-state biofilm develops, possessing a concentration of 1500 mg/dry wt/kg soil near the well bore. A biofilm concentration of 15500 mg dry wt/kg soil is required to plug the pore space fully. Finally, if k_{d1} is set to 0.0044 min^{-1}, measured for 19.7 mg/L porous media reactor data, a steady-state, near-well biofilm concentration of approx 360 mg dry wt/kg soil is observed.

These results indicate that it is important to include biofilm development kinetics in the design of *in situ* bioremediation systems. The primary design constraint that is affected by this parameter is biofouling of nutrient injection wells. Because current bacterial transport theory is not predictive and the detachment rate coefficient changes with substrate loading, it is important to use conservatively low values of k_{d1} based on experimental measurement. Lower values will underpredict detachment and overpredict biofouling. In contrast, other design issues, such as volumetric contaminant destruction and nutrient consumption, are relatively insensitive to bacterial transport parameters, based on these simulations. This is because of the cometabolic kinetics of contaminant destruction and, regardless of value of the detachment coefficient, the glucose was still consumed within 0.4 m of the well bore.

CONCLUSIONS

The ability of published detachment rate expressions to describe experimental results was evaluated. Data were obtained from porous media reactor experiments inoculated with *Ps. aeruginosa* and fed inlet glucose concentrations of 2.3 and 19.7 mg/L. A first-order rate expression on attached biomass concentration gave the best prediction for the combined data sets. However, the value of the detachment rate coefficient was dependent on initial substrate concentration, since k_{d1} values of 9.79×10^{-4} and 4.4×10^{-3} min^{-1} best represented low and high concentration data, respectively. Simulations of the porous media reactor experiments indicate that the response using higher influent substrate concentrations has greater sensitivity to variations in k_{d1}, whereas responses at both substrate concentrations tested are relatively insensitive to changes in the attachment rate parameter k_a. The effects of detachment rate on a field bioremediation system were also estimated using two-dimensional radial simulations. These simulations suggest that biomass profiles in the flow field vary with detachment rate. As a result, biofouling of nutrient injection wells is directly dependent on this parameter. In contrast, simulation results indicate that contaminant destruction and nutrient consumption in the full flow field are not sensitive to the detachment rate. These findings suggest that it is important to include biofilm kinetics in the design of *in situ* bioremediation systems to predict, and possibly minimize, well bore biofouling.

ACKNOWLEDGMENTS

This research was supported by cooperative agreement ECD-8907039 between the National Science Foundation and Montana State University. The portion of this work conducted at the Pacific Northwest Laboratory

was supported by the US Department of Energy Office of Technology Development, VOC-Arid Integrated Demonstration. Pacific Northwest Laboratory is operated for the US Department of Energy by Battelle Memorial Institute under contract DE-AC06-76RLO 1830.

REFERENCES

1. Cunningham, A. B. and Wanner, O. (1993), Modeling microbial processes in porous media with application to biotransformation, *International Symposium on Hydrogeological, Chemical, and Biological Processes of Transformation and Transport of Contaminants in Aquatic Environments*, May 24–29, Rostov-on-Don, Commonwealth of Independent States (the former Soviet Union).
2. Semprini, L., Hopkins, G. D., Janssen, D. B., Lang, M., Roberts, P. V., and McCarty, P. L. (1991), In Situ *Biotransformation of Carbon Tetrachloride under Anoxic Conditions*, EPA Report No. EPA 2-90/060, US EPA, Ada, OK.
3. Shouche, M., Petersen, J. N., and Skeen, R. S. (1993), *Appl. Biochem. Biotechnol.* **39**, 763–779.
4. Roberts, P. V., Hopkins, G. D., Semprini, L., McCarty, P. L., and MacKay, D. M. (1991), Pulsing of electron donor and electron acceptor for enhanced biotransformation of chemicals, US Patent Number 5,006,250. US Patent Office, Washington, DC.
5. Roberts, P. V., Semprini, L., Hopkins, G. D., Grbic-Galic, D., McCarty, P. L., and Reinhard, M. (1989), In Situ *Aquifer Restoration of Chlorinated Aliphatics by Methanotrophic Bacteria*, EPA Report No. EPA 2-89/033 US EPA, Ada, OK.
6. Srinivasan, P. and Mercer, J. W. (1987), *BIO1D Version 1.0 Users Guide*, Geotrans, Inc., Washington, DC.
7. Nichols, W. E. and White, M. D. (1992), *MSTS Multiphase Subsurface Transport Simulator: User's Guide and Reference*, PNL-8637. Pacific Northwest Laboratory, Richland, WA.
8. Wheeler, M. F., Roberson, K. R., and Chilakapati, A. (1992), Three-dimensional bioremediation modeling in heterogeneous porous median, in *Computational Methods in Water Resources IX*, vol. 2, Elsevier, Oxford, UK, pp. 299–315.
9. Taylor, S. W. and Jaffe, P. R. (1990), *Water Resour. Res.* **26(9)**, 2181–2194.
10. Speitel, G. E., Jr., and DiGiano, F. A. (1987), *J. Environ. Eng.* **113(3)**, 464–475.
11. Chang, H. T. and Rittmann, B. E. (1988), *J. WPCF* **60(3)**, 362–368.
12. Bryers, J. D. (1987), *Biotechnol. Prog.* **3(2)**, 57.
13. Stewart, P. S. (1993), *Biotechnol. Bioeng.* **41**, 111–117.
14. Bakke, R., Characklis, W. G., Turakhia, M. H., and Yeh, A.-I. (1990), Modeling a monopopulation biofilm system: *Pseudomonas aeruginosa*, in *Biofilms*, Characklis, W. G. and Marshall, K. C., eds., Wiley, New York, pp. 487–520.
15. Siebel, M. A. and Characklis, W. G. (1991), *Biotechnol. Bioeng.* **37**, 778–789.
16. Cohen, Y. and Metzner, A. B. (1981), *AIChE J.* **27(5)**, 705–715.
17. Taylor, S. W. and Jaffe, P. R. (1990), *Water Resour. Res.* **26(9)**, 2153–2159.

18. Deb, A. K. (1969), *J. Sanit. Eng. Div. Am. Soc. Civ. Eng.* **95(SA3),** 399–422.
19. Kreikenbohm, R. and Stephan, W. (1985), *Biotechnol. Bioeng.* **27,** 296–301.
20. Rittman, B. E. (1989). Detachment from biofilms, in *Structure and Function of Biofilms,* Characklis, W. G. and Wilderer, P. A., eds., Wiley, New York, pp. 49–58.
21. Trulear, M. G. and Characklis, W. G. (1982), *J. WPCF* **54(9),** 1288–1301.
22. Wanner, O. and Gujer, W. (1986), *Biotechnol. Bioeng.* **28,** 314–328.
23. Chiang, C. Y., Dawson, C. N., and Wheeler, M. F. (1990), *Modeling of* In-situ *Biorestoration of Organic Compounds in Groundwater,* Technical Report TR90-31. Rice University, Houston, TX.
24. Chiang, C. Y., Wheeler, M. F., and Bedient, P. B. (1989), *Water Resour. Res.* **25,** 1541–1549.
25. Peyton, B. M. and Characklis, W. G. (1993), *Biotechnol. Bioeng.* **41,** 728–735.
26. Hooker, B. S., Skeen, R. S., and Petersen, J. N. (1994), *Biotechnol. Bioeng.* in press.
27. Taylor, S. W., Miller, P. C. D., and Jaffe, P. R. (1990), *Wat. Resour. Res.* **26(9),** 2161–2169.